RSC Advances

ROYAL SOCIETY OF CHEMISTRY

www.rsc.org/advances

Diverse silver(I) sulfobenzoate coordination polymers and their recycling property as homogeneous catalyst in oxygenation of sulfide

Ai-Qing Ma and Long-Guan Zhu*
Department of Chemistry, Zhejiang University, Hangzhou 310027, People's Republic of China
E-mail:chezlg@zju.edu.cn

Four diverse silver(I) coordination polymers have been synthesized and fully characterized by elemental analysis, powder X-ray analysis, IR spectra, TG analysis, fluorescence study, and single crystal X-ray analysis, namely $\{[Ag_3(bpmb)_{2.5}(2\text{-}sb)(2\text{-}Hsb)]\cdot(0.5H_2O)\}_n$ (**1**), $[Ag_2(bpmb)_3(2\text{-}Hsb)_2]_n$ (**2**), $\{[Ag_2(bpmb)_2(3\text{-}sb)]\cdot 4H_2O\}_n$ (**3**), and $\{[Ag(bpmb)(4\text{-}Hsb)]\cdot 2H_2O\}_n$ (**4**) where bpmb is 1,4-bis(pyrazolyl-methyl)-benzene and sb is sulfobenzoate dianion. In these complexes, bpmb ligand plays the role of bidentate bridge linking with silver ions, while the sb ligands display versatile coordination modes. The combination of the two ligands manages the silver ions to give rise to a variety of coordination networks in **1**-**4**. The accessorial secondary interactions such as hydrogen bonding in complexes **1**-**4** and aromatic stacking in complexes **1**-**3** are also helpful for the extension and stabilization of the final supramolecular aggregates. Moreover, the catalytic activity to selective oxidation of methyl phenyl sulfide with H_2O_2 to sulfoxide also has been carried out. Complexes **2** and **4** afforded 98% and 96% conversion with 93% and 90 selectivity for the methyl phenyl sulfoxide in 3 h at 323K, respectively. Especially, complex **2** is a homogeneous catalyst during the catalytic reaction while it can be recovered by filtration upon cooling and then reused at least four times without losing activity, which is very rare in the oxygenation of sulfide.

Introduction

Crystal engineering of construction design and rational synthesis of coordination polymers based on the interactions of metal ions with organic ligands,[1] is a popular area of current research[2] in recent decades owing to their intriguing aesthetic structures and topological features as well as their potential applications in magnetism, electric conductivity, molecular adsorption, heterogeneous catalysis, nonlinear optics and fluorescent materials.[3-7] Coordination polymers developed from silver ions and heterocyclic nitrogen ligands continue to attract attention due to the coordinative sphere of the d^{10} silver(I) ion is varied from 2 to 6 and various geometries (linear, trigonal, tetrahedral, trigonal, pyramidal, and octahedral).[8-11] The supramolecular chemistry of Ag(I) coordination polymers represents a dynamic and thriving field which abounds with various supramolecular forces such as metal-ligand, metal-π, and metal-metal interactions, hydrogen bonds, π-π stacking, and anion interactions.[10, 12-14] Therefore the crystallization of Ag(I) complexes would depend on the delicate balance of thermodynamic and kinetic contributions concerning synergetic supramolecular interactions, which may account for the fact that the structures and topologies of Ag(I) complexes can be astonishingly varied even with similar ligands.[12,15-16] Sulfobenzoates with sulfonate and carboxylate groups are useful synthetic synthons which can develop multimodal and polydentate coordinative systems. The silver coordination complexes with several sulfobenzoates have also been reported in our group and in some of these cases interesting polymeric systems have been structurally characterized.[16-17] However, reports on the coordination complexes based on the sulfobenzoates with various N-donor ligands are still limited.[18-19] In addition, our team has recently focused on the catalytic activity of the metal-organic coordination complexes with sulfobenzoates as ligands and has explored the catalytic activity of the oxidation reaction of methyl phenyl sulfide (MPS).[20] Sulfoxides are important in organic chemistry,[21-23] owing to their versatile usage as intermediates or products in the synthesis of pharmaceuticals, agrochemicals, and other fine chemicals.[24-25] Some silver salts including $AgNO_3$ have been reported to convert sulfides into sulfoxides.[26] However, these salts suffer from low activity even with long time under a higher temperature. Our initial research on transition metal sulfobenzoate complexes exhibited the catalytic activity on the oxidation of MPS[20] and the sulfobenzoate ligand can promote the solubility of the complexes. Therefore the combination of sulfobenzoate and silver is expected to have catalytic activity on MPS. Here, this paper describes synthesis, crystal structures, and catalytic properties of four complexes, namely $\{[Ag_3(bpmb)_{2.5}(2\text{-}sb)(2\text{-}Hsb)]\cdot(0.5H_2O)\}_n$ (**1**), $[Ag_2(bpmb)_3(2\text{-}Hsb)_2]_n$ (**2**), $\{[Ag_2(bpmb)_2(3\text{-}sb)]\cdot 4H_2O\}_n$ (**3**), and $\{[Ag(bpmb)(4\text{-}Hsb)]\cdot 2H_2O\}_n$ (**4**) (sb = sulfobenzoate dianion, bpmb = 1,4-bis(pyrazolyl-methyl)-benzene).

Results and Discussion

Reaction Chemistry and XRD Study for Complexes 1-4

To get these complexes, different methods and starting materials have been explored. For complexes **1**-**3**, CH_3COOAg was used as the starting material by the combination of hydrothermal method and solvent evaporation, while complex **4** was directly synthesized from the cooling solution of the reaction system used $AgNO_3$ as the starting material. Another emphasis we should notice is the different molar ratio in the reaction. If the molar ratio of CH_3COOAg:2-H_2sb:bpmb was fixed at 2:2:1at 393 K, complex **1** was obtained, while the ratio of starting materials changed to 1:1:1 with the same other conditions, complex **2** could be achieved. The synthesis of complexes **1** and **2** is only different in the molar ratio and the quantity of starting materials. The environmental synthetic condition for complex **1** was at a lower concentration for starting materials and lower molar ration of Ag: bpmb. Therefore, these two factors led to the preparation of two diverse complexes. Complex **3** was obtained by a procedure similar to that of **2** except using 3-NaHsb instead of 2-H_2sb. Compared with **1**-**3**, complex **4** was synthesized under higher temperature of 423K. Moreover complexes **1**-**3** were obtained in the solvent mixture of water and acetonitrile, while complex **4** was obtained only using water as the solvent in the synthetic process.

Based on the above synthetic information, we can conclude that the starting materials, pressure, temperature, solvent, synthetic conditions, especially molar ratio are so important in the synthesis of complexes **1-4**, which may be mainly attributed to the coordination property of the sb ligands, since sb has two different functional groups and their coordination abilities are largely influenced by the external stimuli such as synthetic conditions.

These complexes were separated only as single crystals without any powder. The purities of these complexes were further confirmed by XRD analysis, in which the experimental XRD patterns are good consistent with those obtained from the single crystal data at room temperature (See supporting information, Figures S1-S8). The only difference in reflection intensities between the simulated and experimental patterns was due to the variation in preferred orientation of the powder samples during the collection of the experimental XRD data.

X-ray Crystallography

Complex **1** is a two-dimensional structure constructed from Ag(I), bpmb, 2-Hsb$^-$, 2-sb^{2-}, and lattice water molecules. There are three silver ions in an asymmetric unit as shown in Figure 1 and two 2-sb ligands exist in two forms, one is fully deprotonated and the other is partly deprotonated (a and b in Scheme 1). The coordination spheres of all Ag ions can be described as tetrahedral geometry. Ag1 adopts two nitrogen atoms from two bpmb ligands and two oxygen atoms from the carboxyl group (O1) of the 2-Hsb$^-$ and the sulfonate group (O10) of the 2-sb^{2-}. Ag2 is coordinated to one nitrogen atom from one bpmb ligand and three oxygen atoms from the carboxyl group (O1 and O2) of the 2-Hsb$^-$ and the sulfonate group (O8) of 2-sb^{2-} ligands. Ag3 is a tetrahedron coordination geometry completed by two nitrogen atoms from two bpmb and two oxygen atoms from the μ_3-carboxyl group and the μ_2-sulfonate group (O3) of the 2-sb^{2-} ligand. Ag1 and Ag2 are bridged by the sulfonate group of the 2-Hsb$^-$ and the carboxyl group of the 2-sb^{2-} with the Ag…Ag distance of 3.6833(6) Å. The Ag2 and Ag3 are bridged by the carboxyl of the 2-sb^{2-} with the Ag…Ag distance of 4.0428(5) Å. The 2-sb^{2-} ligand coordinates to Ag1, Ag2 and Ag3 through the carboxyl and sulfonate groups. The bpmb ligands link both Ag2 and its symmetric one and both Ag1 and Ag3. Therefore 2-sb^{2-} and bpmb extend the structure into 2-D architecture (Figure S9).

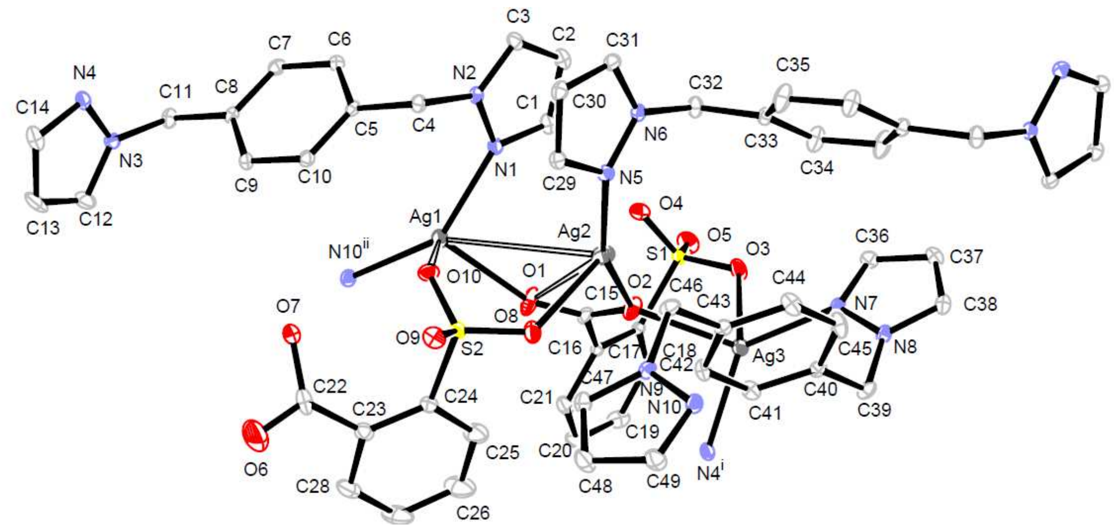

Figure 1 ORTEP view of the asymmetric unit of complex **1** with numbering scheme and the probability is drawn at 30%. The H atoms and lattice water molecule are omitted for clarity. Symmetry codes, i: -1+x, 1+y, z; ii: 1+x,y,z.

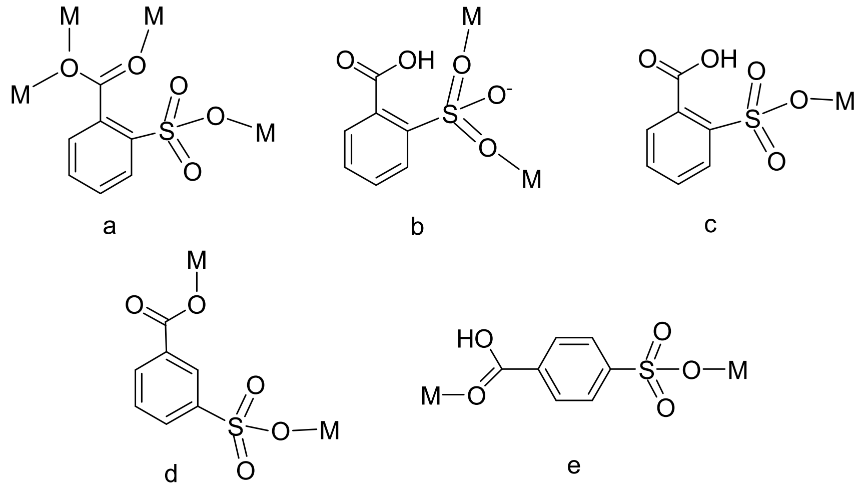

Scheme 1 The coordination modes of sb ligands in complexes **1-4**

Table 1 Selected bond lengths (Å) and angles (°).

Complex **1**			
Ag1-O1	2.349(3)	Ag1-O10	2.705(3)
Ag1-N1	2.215(3)	$Ag1-N10^{ii}$	2.190(3)
Ag2-O1	2.904(5)	Ag2-O2	2.183(3)
Ag2-O8	2.588(4)	Ag2-N5	2.178(3)
Ag3-O2	2.396(3)	Ag3-O3	2.542(3)
$Ag3-N4^{i}$	2.275(4)	Ag3-N7	2.209(3)
O1-Ag1-O10	101.26(11)	O1-Ag1-N1	96.03(15)
$O1-Ag1-N10^{ii}$	112.23(15)	O10-Ag1-N1	96.14(11)

O10-Ag1-N10^{ii}	100.30(11)	N1-Ag1-N10^{ii}	143.45(12)
O1-Ag2-O2	48.09(11)	O1-Ag2-O8	91.50(12)
O1-Ag2-N5	142.27(11)	O2-Ag2-O8	111.73(13)
O2-Ag2-N5	156.81(14)	O8-Ag2-N5	90.38(12)
O2-Ag3-O3	86.37(12)	O2-Ag3-N4^{i}	93.86(12)
O2-Ag3-N7	131.44(12)	O3-Ag3-N4^{i}	120.95(12)
O3-Ag3-N7	85.52(11)	N4^{i}-Ag3-N7	130.61(12)
Complex **2**			
Ag1-O3	2.8195(19)	Ag1-N1	2.300(2)
Ag1-N3	2.245(2)	Ag1-N5	2.269(2)
O3-Ag1-N1	98.55(7)	O3-Ag1-N3	101.11(7)
O3-Ag1-N5	82.38(7)	N1-Ag1-N3	115.81(8)
N1-Ag1-N5	112.15(8)	N3-Ag1-N5	130.64(8)
Complex **3**			
Ag1-O1	2.299(3)	Ag1-O1w	3.001(4)
Ag1-N1	2.257(3)	Ag1-N3	2.234(3)
Ag2-O4	2.612(4)	Ag2-N5	2.113(3)
Ag2-N8^{ii}	2.109(3)		
O1-Ag1-O1w	94.04(11)	O1-Ag1-N1	113.04(11)
O1-Ag1-N3	120.92(12)	O1w-Ag1-N1	107.38(11)
O1w-Ag1-N3	76.67(11)	N1-Ag1-N3	125.53(11)
O4-Ag2-N5	100.40(13)	O4-Ag2-N8^{ii}	89.64(12)
N5-Ag2-N8^{ii}	169.24(13)		
Complex **4**			
Ag1-O2^{i}	2.883(3)	Ag1-O3	2.612(3)
Ag1-N1	2.151(3)	Ag1-N3	2.148(3)
O2^{i}-Ag1-O3	87.26(12)	O2^{i}-Ag1-N1	86.20(10)
O2^{i}-Ag1-N3	100.22(11)	O3-Ag1-N1	112.03(12)
O3-Ag1-N3	86.61(12)	N1-Ag1-N3	160.69(12)

Symmetry codes: in **1**: i: -1+x, 1+y, z; ii: 1+x,y,z.; in **3**, i, -x, 2- y, 1-z; ii: x, 1-y, 1-z; iii: -x, 1-y, -z.; in **4**, x,-1+y,z.

The single crystal X-ray analysis revealed that complex **2** consists of Ag(I), bpmb, and 2-Hsb^{-} (Figure 2 and c in scheme 1), which is very different from that of **1**. In the asymmetric unit, there is only one Ag(I) ion and its coordination geometry is a tetrahedron completed by three N donors from three bpmb ligands and one O atom from the sulfonate group (O3) with a longer distance of 2.8195(19) Å (Figure 2 and

Table 1). In complex **2**, the bpmb ligands adopt bridging bidentate coordination fashion, forming a 2-D framework (Figure S10).

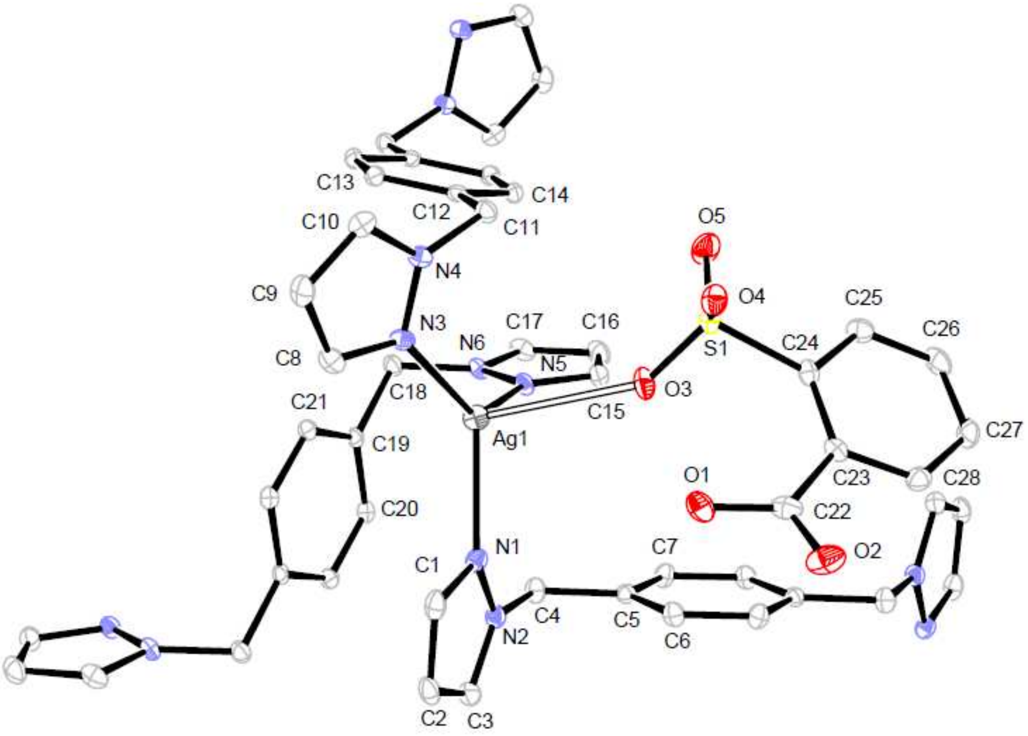

Figure 2 ORTEP view of the asymmetric unit of complex **2** with the numbering scheme. The thermal ellipsoids are drawn at 30% probability. The weak bond is represented as open line. The H atoms are omitted for clarity.

Complex **3** consists of silver ions, 3-sb^{2-}, bpmb, and lattice water molecules. There are two silver ions in an asymmetric unit shown in Figure 3. Ag1 is surrounded by two nitrogen atoms from two bpmb ligands and two oxygen atoms from one carboxyl group and one water molecule with a longer distance of 3.001(4) Å (Table 1). Ag2 is a T-shaped coordination geometry completed by two nitrogen atoms from two bpmb ligands and one oxygen atom from one sulfonate group (O4). The 3-sb^{2-} ligand bridges Ag1 and Ag2 through carboxyl and sulfonate groups (d in Scheme 1). The bpmb ligands also act as bridging ligand, connecting to two silver ions. The molecular structure of **3** is a 2-D architecture (Figure S11).

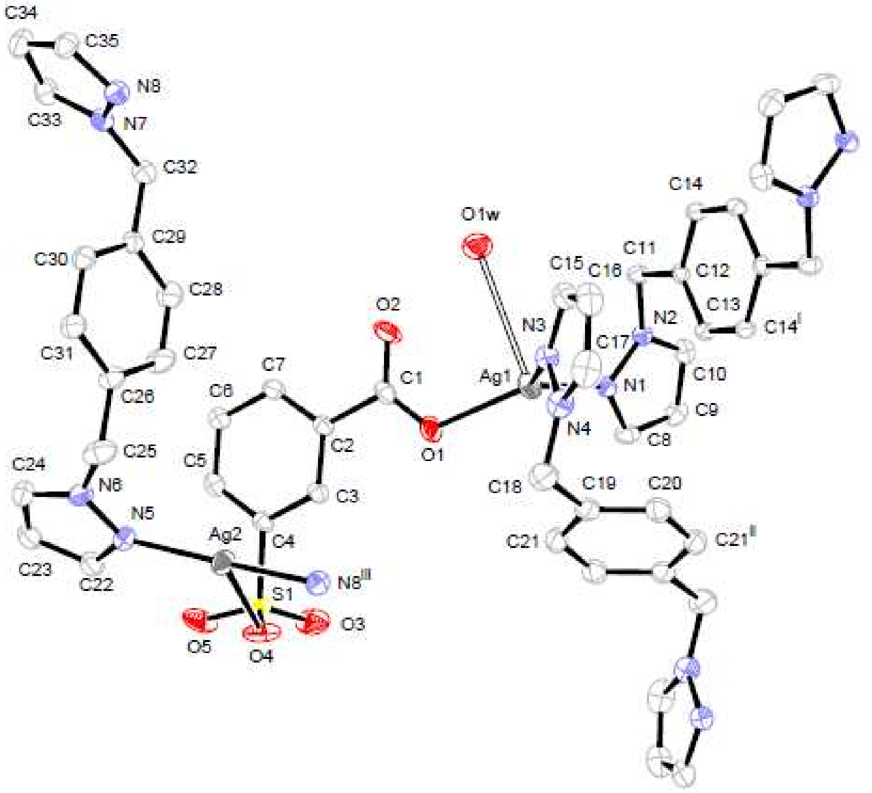

Figure 3 ORTEP view of the asymmetric unit of complex **3** with the numbering scheme. The thermal probability is drawn at 30%. H atoms and lattice water molecules are omitted for clarity. The weak bond is represented as open line. Symmetry codes: i, -x, 2- y, 1-z; ii: x, 1-y, 1-z; iii: -x, 1-y, -z.

The asymmetry unit of complex **4** contains one silver ion, one 4-Hsb$^-$ ligand, one bpmb ligand, and two lattice water molecules (Figure 4 and e in Scheme 1). Ag1 is in a distorted tetrahedral geometry completed by two nitrogen atoms from two bpmb ligands and two oxygen atoms from two 4-Hsb$^-$ ligands [one is from carboxyl group and the other is from sulfonate group (O3)] with a longer distance of 2.883(3) Å (Table 1). Both bpmb and 4-Hsb$^-$ ligands act as bridging linkers to extend the structure into 2-D layer (Figure S12).

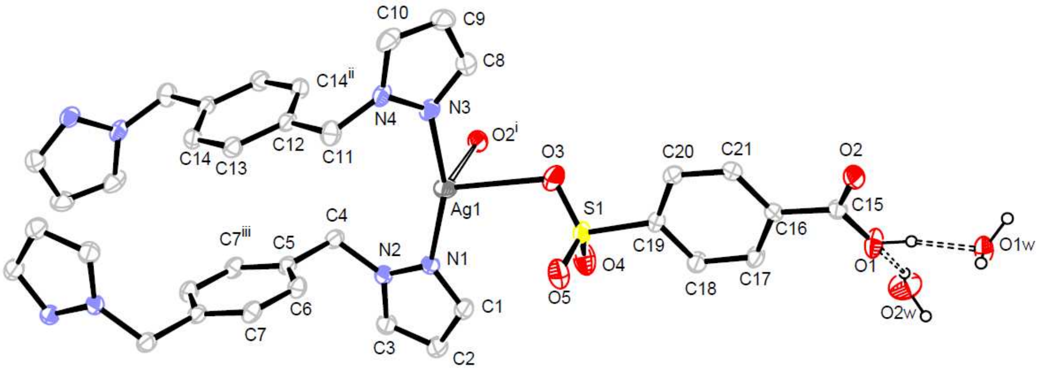

Figure 4 ORTEP view of the asymmetric unit of complex **4** with the numbering scheme. The probability is drawn at 30%. The weak bond is represented as open line and the hydrogen bonds are represented as dashed lines. Symmetry codes, i:x,-1+y,z;ii:2-x,1-y,1-z;iii:1-x,1-y,1-z.

Hydrogen bonds, C-H…aromatic interactions, and C-H…O interactions exist in all these complexes. The aromatic stacking effects only exist in complexes **1-3** and in **2** this interaction is weak.

Thermal stability

Thermo-gravimetric analysis (TGA) was conducted to study the stability of four complexes (Figure 5). The TGA curve for complex **1** has three degradation steps in the range 42–750°C. The first gradual weight loss of 0.70% occurs between 42 and 175°C (calculated 0.68%), corresponding to the loss of the half water molecule per formula unit. In the temperature range 186-312°C complex **1** lost weight of 29.58% without a clear platform, corresponding to the release of the two coordinated sb ligands (calculated 30.18%). Compared with **1**, complex **2** is stable up to ca. 210°C, and the first-step weight loss of 14.72% in the temperature range 210-270°C for the release of one sb ligand (calculated 15.11%) without a clear platform, and then a successive decomposition step occurs, which is attributed to loss of the sb and bpmb ligands. For complex **3**, the first weight loss of 7.47% occurs between 25 and 120°C (calculated 7.47%), corresponding to the loss of the four guest water molecules. Then, complex **3** started to decompose at 190°C. Complex **4** began to lose weight of 6.22% (calculated 6.17%) in the temperature range 25-150°C, which is accounted for the liberation of two lattice water molecules. And complex **4** decomposed at 240°C. The thermal stability for four complexes has some different. Complexes **1**, **3**, and **4** contain solvents and they lost weight at low temperature. Complex **2** has no any solvent and the decomposition temperature at 210°C. Complexes **1** and **2** contain same ligands of bpmb and 2-sulfobenzoate, while the existence forms of 2-sulfobenozate ligands in both complexes are different and their coordination modes also different. Therefore complex **2** and desolvented **1** have somewhat different decomposition temperature. Desolvented complexes **1**, **3** and **4** have different sulfobenzoate ligands and these sulfobenzoate ligands exhibit different coordination modes, leading to some different decomposition temperatures.

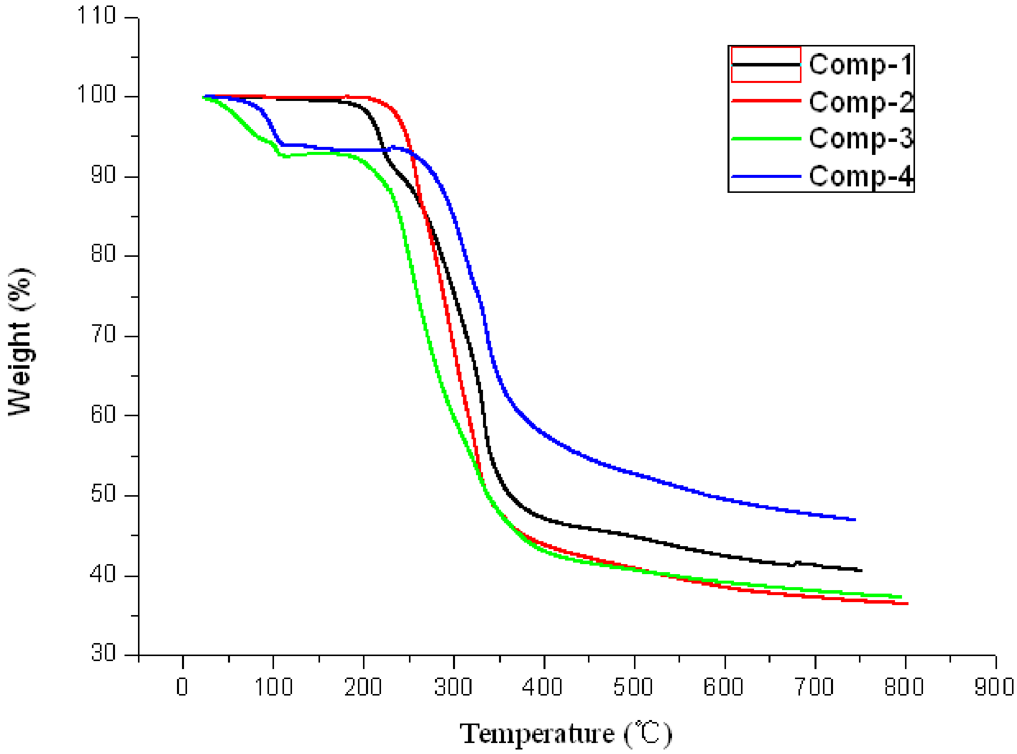

Figure 5 TGA curves of complexes **1**–**4**.

UV spectra analysis

The UV-vis spectra were measured in methanol with the concentration of 2.22×10^{-5} mol/L. These complexes have more intensive absorptions than those of free ligands, indicating that the coordination of ligands can enhance the absorptions (Figure 6 and Table 2). Absorptions of complexes **1-2** with 2-sb ligand are slightly stronger than those of **3-4**, while the absorption of 2-H_2sb ligand is weaker than those of 3-NaHsb and 4-KHsb ligands, indicating that the coordination has a significant influence on the absorptions of 2-H_2sb. The shifts of adsorption peaks in four complexes are controlled by many factors, such as solvent effect, conjugation, super-conjugation, steric hindrance, and the ligand type in complexes. The peak near 220 nm for complexes **1-3** are red-shifted compared with corresponding ligands. However, complex **4** has a distinct blue shift in comparison with 4-KHsb at 234 nm. This may be ascribed to that the para-position of sulfonate in complex **4** plays an important role in better conjugation although the electronic effect of ortho-position of **1** and para-position of **4** are similar. Better conjugation results in lower energy level of basic state of electron. Consequently energy level difference is bigger and blue shift takes place in complex **4**. The bands at 253 nm in **1**, 283 nm in **2**, and 285 nm in **3** are the results of metal-to-ligand charge transfer (MLCT) are observed.

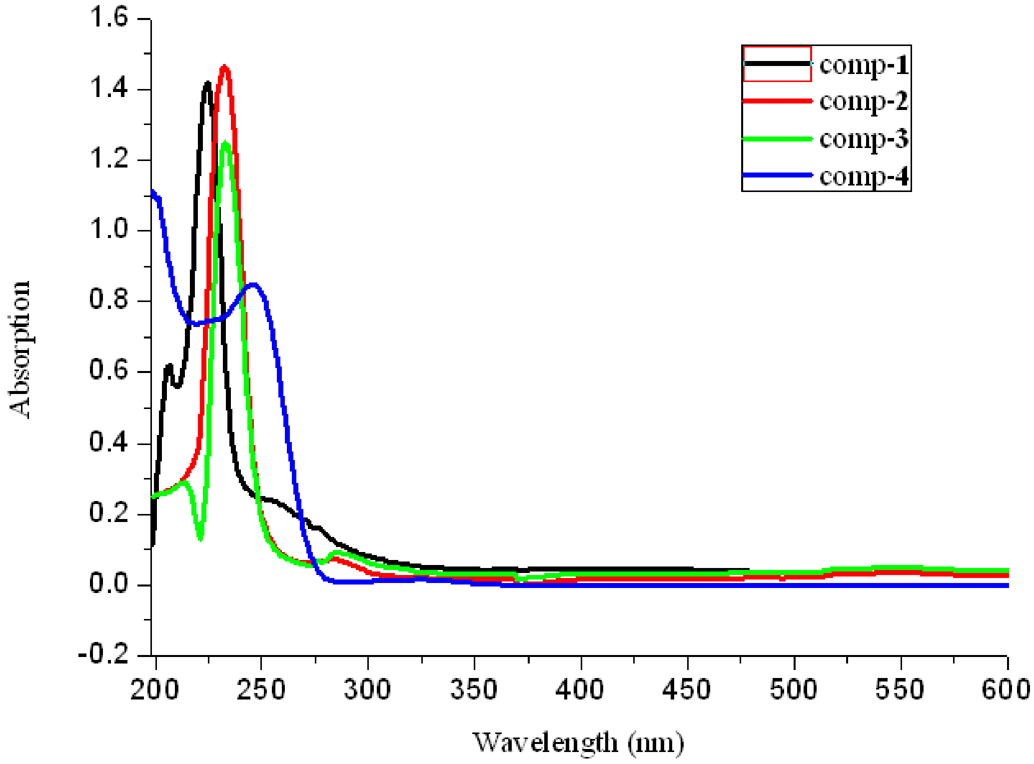

Figure 6 UV-vis spectra of complexes **1**–**4** in methanol.

Table 2 UV-vis absorption spectral data for complexes **1**–**4** in methanol with the concentration of 2.22×10^{-5} mol/L.

Complex	λ_{max}/nm (ε/dm^3.mol^{-1}.cm^{-1})		
1	253 (1.09×10^4)	224 (6.38×10^4)	207 (2.79×10^4)
2	283 (0.33×10^4)	232 (6.59×10^4)	
3	285 (0.42×10^4)	233 (5.63×10^4)	
4	246 (3.82×10^4)	222(3.820×10^4)	201 (4.92×10^4)

Fluorescence property

The solid-state fluorescent properties of complexes **1**–**4** have been investigated at room temperature, as depicted in Figure 7. The maximum emissions for these complexes occur at 389 nm ($\lambda_{e\ x}$= 240 nm), which is similar to those of the acidic and neutral ligands, showing that the coordination does not affect the fluorescent emissive position dramatically. While the strengths of the four complexes are all obviously lower than the corresponding ligands, and especially they almost quench the emission at 289 nm, at which the bpmb ligand has a strong emission. The reason for the intensity reduction or even quenching probably is due to the introduction of the metal ions and solvent molecules, which play an important role in weakening the fluorescent emission.[28-30] Meanwhile, the weak interactions, especially the hydrogen-bonding interactions, also play an important role in weakening the fluorescence intensity of the supermolecules.[31-32] It is also worth noting that the different coordination modes of 2-sb may result a small different intensities in complexes **1** and **2**.

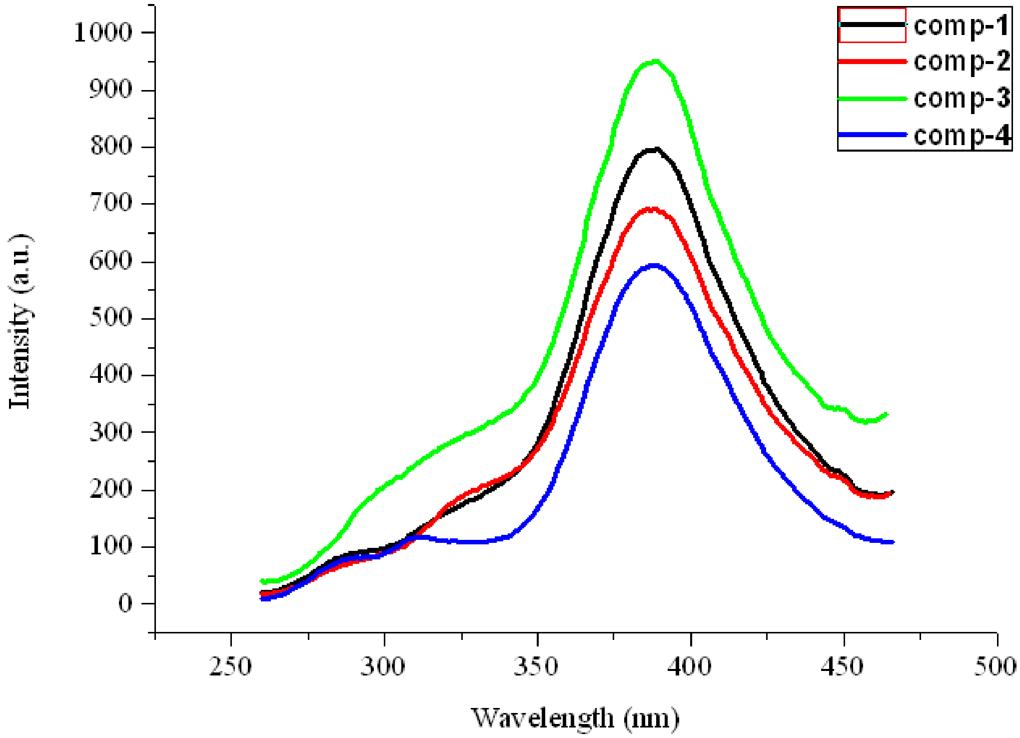

Figure 7 Solid-state emission spectra for complexes **1–4.**

Catalytic activities

The catalytic activities of four complexes in the oxidation of methyl phenyl sulfide (MPS) at 50°C were investigated (Scheme 2). The results indicated that the structures of the complexes are largely related to the catalytic activity of the oxidation of MPS. Catalysts **2** and **4** are more active than those of **1** and **3** (Figure 8). The acid can promote the conversion of the oxidation of MPS.[33] Therefore, the 2-H_2sb (2 mol% vs. MPS) was introduced into the reaction system, and the experimental results are shown in Figure 9. Complexes **2** and **4** both are highly efficient and selective catalysts (Table 3). Moreover, complex **2** can be reused at least four times (Figure 10) without losing activity and show no significant difference with the fresh one in the XRD patterns (Figures S13-14). These four complexes are composed of silver, bpmb, and sulfobenzoate ligands, and they exhibited large different catalytic activity on the oxidation of MPS. Complex **2** has the highest catalytic activity, but it should be used as catalyst with the 2-H_2sb. Their catalytic activity largely depends on the several factors, such as the amount of oxidant, solvent, temperature, and the nature of the catalyst. Complexes **1** and **3** are nearly insoluble in ethanol solvent, while complexes **2** and **4** are both gradually dissolved in the mixture with the reaction going on as homogenous catalysts at reaction temperature (50°C), and after cooling to the room temperature complex **2** could be separated out by simple filtration (the recycling quantity is about 80%). Therefore complexes **1** and **3** can be used as heterogeneous catalysts, while complexes **2** and **4** can be used as homogeneous catalysts. Complex **4** could not be precipitated from the reaction solution. As a result, only complex **2** can be reused. The 2-H_2sb as a catalyst performed below 80% conversion and could not be promoted further. The combination of the neat complex **2** and 2-H_2sb can exhibit the cooperative effect with the conversion of 98% due to the 2-H_2sb can provide the acidic environment. The electron-rich sulfur atom of the MPS undergoes electrophilic oxidation by H_2O_2 to produce the sulfoxide and sulfone, which suggests that the acidic environment is benefit for the oxidation of MPS and the titration experiment further confirmed the formation of intermediates with proton.[34] In the early stage, people used strong acid as a reagent to oxidize the MPS, but such system brought about the environmental pollution. Therefore now people use H_2O_2 as oxidant to oxidation of MPS under suitable catalyst. These four complexes could not provide some acidity and the combination of complex **2** and 2-H_2sb with moderate acidity can significantly exert the catalytic activity. In our previous reports on Ru and Pd sulfobenzoate complexes,[35] the 2-sb complexes also exhibited the higher catalytic activity than those of 3-sb or 4-sb metal complexes, suggesting that the ortho position of the sulfo group provides better conjugation leading to dominance in catalyzed oxidation. The complex **2** as a catalyst under the cooperative effect by 2-H_2sb in the oxidation of MPS is the first recyclable homogeneous catalyst with excellent catalytic activity.

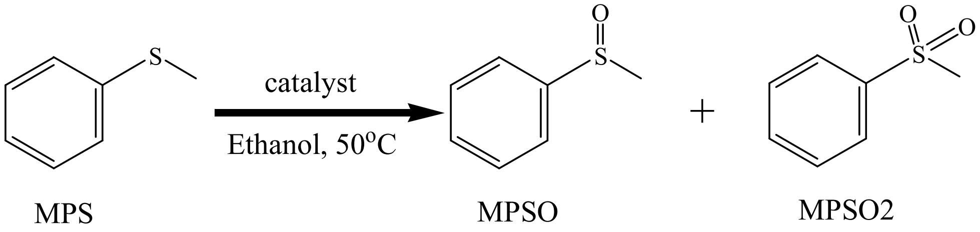

Scheme 2 The oxidation of MPS.

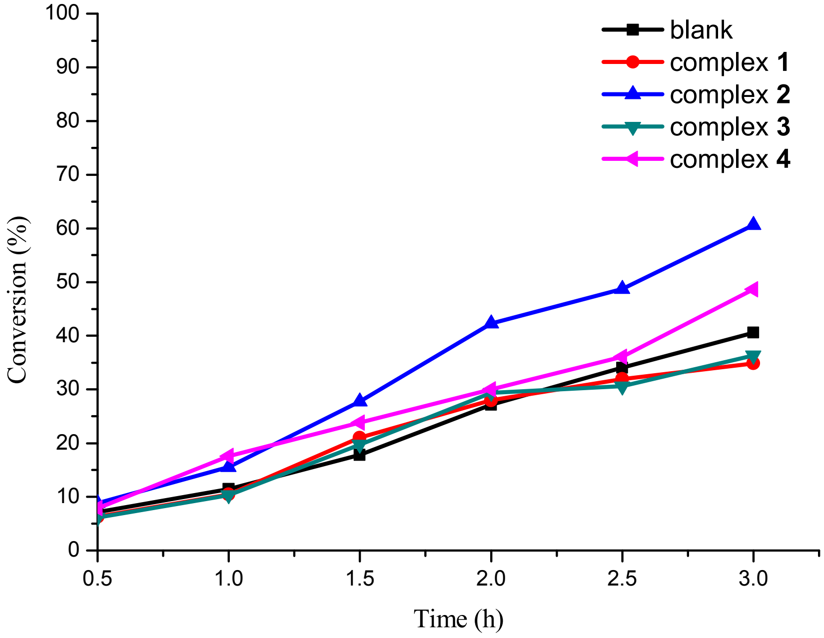

Figure 8 The conversion of MPS vs reaction time plot for the oxidation of MPS by complexes **1-4**. Blank experimental conditions: 0.5 mmol of MPS and 1.5 mmol of H_2O_2 were mixed in 5 mL of ethanol at 50°C. The representative GC chromatograms are presented in Supporting Information (Figures S15-21).

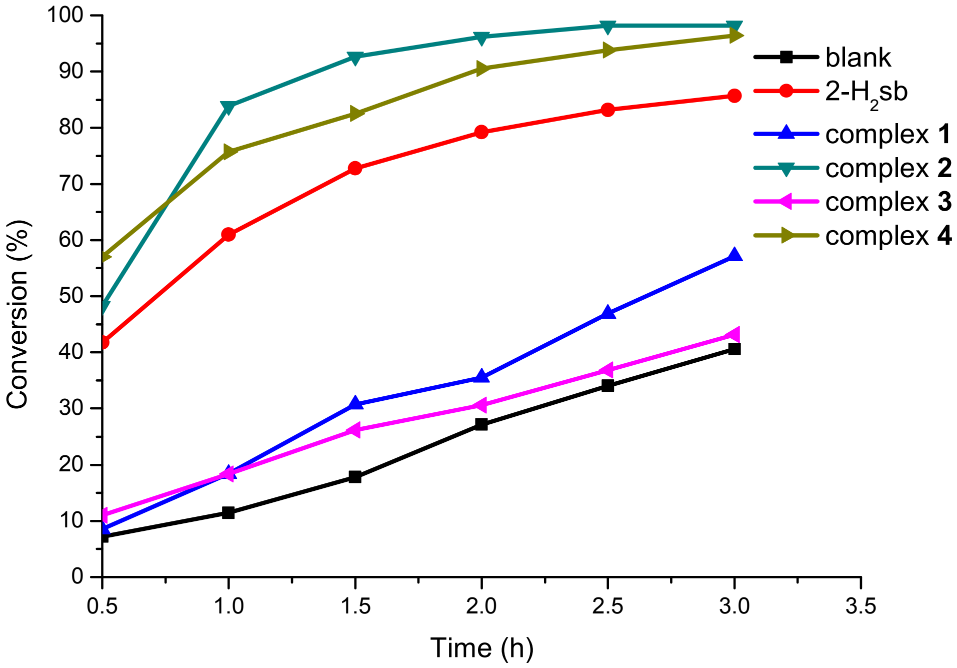

Figure 9 The conversion of MPS vs reaction time plot for the oxidation of MPS by complexes **1-4** in the present of 2-H_2sb.

Table 3 The results of the oxidation of methyl phenyl sulfide by complexes **1-4**.

complex	Time/h	Conversion/%	Selectivity for MPSO/%
1	3	35	86
2	3	77	94
3	3	37	91
4	3	53	90
1+2-H_2sb	3	57	93
2+2-H_2sb	3	98	93
3+2-H_2sb	3	43	90
4+2-H_2sb	3	96	91
2-H_2sb	3	79	96
blank	3	40	82

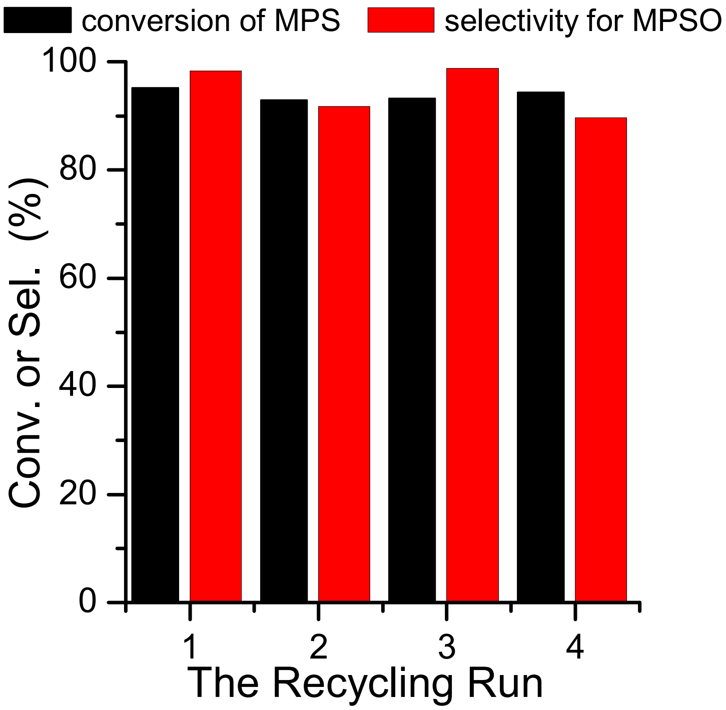

Figure 10 Catalytic activities of four recycling runs for complex **2**.

Conclusion

In summary, we have successfully synthesized four silver sulfobenzoate coordination polymers with bpmb ligand. The variable positions of sulfonate groups on benzene rings give rise to different coordination polymers and variable chemistry properties. The 2-sb ligand yields more abundant coordination modes. Complexes **2** and **4** demonstrated high efficiency and good selectivity in the oxidation of MPS to the corresponding sulfoxide using H_2O_2 as the oxidant. The results indicate that these catalysts have higher catalytic activities than those silver salts or other transition metal catalysts. The sulfonate group can promote the solubility in polar solvents and this specific character largely helps the complex can act as homogenous catalyst but can be recovered by simple cooling for complex **2**, which is an excellent example for the recycling homogeneous catalysts.

Experimental Section

General Information

Chemicals were purchased from commercial sources and were used without further purification. C, H, and N elemental analyses were carried out on a Perkin-Elmer analyzer model 1110. The IR spectra were obtained on a Nicolet Nexus 470 infrared spectrophotometer in KBr pellets in the 400-4000 cm^{-1} region. The fluorescence spectra were measured in powder sample using SHIMADZU RF-540 spectrometer at room temperature. Thermogravimetric analyses (TGA) were carried out using a Delta Series TA-SDT Q600 in nitrogen flow in the temperature range room temperature to

800°C at a heating rate of 10°C/min with Al_2O_3 crucibles. The UV-vis spectra were performed on a Varian Bio 2550 UV-visible spectrophotometer in CH_3OH at room temperature. ^1H and ^{13}C NMR spectra were recorded on a Bruker NMR AVANCE^{III} 400 or 500 spectrometer. The powder X-ray diffractions were measured by Rigaku D/MaX 2550PC with Cu-Kα radiation. The GC data were recorded on a Fuli Gas Chromatography equipped with a DB-5 capillary column. All the standard substances used in GC were purchased from Alfa Aesar. The retention times for the assignment of GC peaks for sulfide, sulfoxide and sulfone are about 4.6 min 7.8 min, and 8.5 min, respectively under following conditions. Detector: FID, 220°C; Sample injector: splitless, 200°C; Column temperature: temperature programming with heating rate of 15 °C/min, initial temperature of 100°C for 3 min and final temperature of 200°C for 2 min.

Synthesis of 1,4-bis (pyrazolyl–methyl)-benzene (bpmb)

1,4-Bis (pyrazolyl–methyl)-benzene (bpmb) was synthesized by one step according to the reference.[36] Pyrazole (9.032 g, 0.13 mol), α,α'-dichloro-p-xylene (10.52 g, 0.065 mol), and tetrabutyl ammonium bromide (1.024 g, 3 mmol) were mixed in benzene (600 mL), and then 100 mL 40% NaOH solution was added under stirring. The mixture was refluxed for about 24 h. After removing benzene by rotator, yellow powder was obtained, which was dissolved in ethyl acetate and re-crystallized at room temperature. After further twice re-crystallization, white crystalline product was obtained. ^1H NMR [DMSO-d_6, 25 °C, 500 MHz; δ(ppm)]: 7.79 (d, *J*=5.0 Hz, 2H), 7.44 (d, *J*=5.0 Hz, 2H), 7.16 (s, 4H), 6.25 (t, *J*=5.0 Hz, 2H), 5.29 (s, 4H).

Synthesis of $\{[Ag_3(bpmb)_{2.5}(2\text{-}sb)(2\text{-}Hsb)]\cdot(0.5H_2O)\}_n$ (1)

A mixture of CH_3COOAg (0.032 g, 0.20 mmol), 2-H_2sb (0.042g, 0.20 mmol), bpmb (0.029 g, 0.12 mmol), distilled water (13 ml) and acetonitrile (3 ml) was placed in a 30-mL Teflon lined stainless-steel reactor and heated at 393 K for two days. After cooling to the room temperature, a clear solution was obtained and then filtered. The resulting solution was set in the dark for evaporation. Two days later, colorless block-shaped crystals were collected by filtration. Yield: 67%. Anal. Calcd (%) for $C_{98}H_{90}N_{20}Ag_6S_4O_{21}$: C, 44.28; H, 3.38; N, 10.54. Found: C, 44.32; H, 3.33; N, 10.49. IR (KBr pellet, cm^{-1}): 3519 (m), 3106 (s), 2937(m),1731(s) , 1587 (s), 1560 (s), 1517(m),1438 (s), 1424(s),1405 (s), 1370 (s),1271 (s), 1258(s),1183 (s), 1095 (s), 1080(s), 1060 (s), 1014(s), 979 (m), 919(w), 843 (m), 808(m), 786 (s), 756(s), 727 (s), 614 (s), 567(m). ^1H NMR [DMSO-d_6, , 25 °C, 400 MHz; δ(ppm)]: 14.17 (s, 1H), 7.92–7.79 (m, 7H), 7.47–7.39 (m, 11H), 7.18 (s, 10H), 6.31 (t, *J*=5.0Hz, 5H), 5.33ppm (s, 10H). ^{13}C NMR [DMSO-d_6, 25 °C, 400 MHz; δ(ppm)]: 140.0, 136.7, 131.0, 129.3, 127.8, 126.8, 105.7, 54.4.

Synthesis of $[Ag_2(bpmb)_3(2\text{-}Hsb)_2]_n$ (2)

The synthesis of **2** was similar to that described for **1**, except for the different molar ratio for starting materials and heating time. A mixture of CH_3COOAg (0.065 g, 0.40 mmol), 2-H_2sb (0.084g, 0.40 mmol), bpmb (0.095 g, 0.40 mmol), distilled water (13 ml) and acetonitrile (3 ml) was placed in a 30-mL Teflon lined stainless-steel reactor and heated at 393 K for 36h. After cooling to the room temperature, a clear solution was obtained and then filtered. The resulting solution was allowed to evaporate in the dark for two days. Then colorless plate-like crystals were collected by filtration. Yield: 76%. Anal. Calcd (%) for $C_{56}H_{52}N_{12}Ag_2S_2O_{10}$: C, 50.53; H, 3.76; N, 12.63. Found: C, 50.30; H, 3.83; N, 12.52. IR (KBr pellet, cm^{-1}): 3519 (m), 3117 (s), 2935(m),2656(w),1716(s), 1589 (w), 1518(s),1438 (s), 1424(s),1400 (s), 1358(m),1286 (s), 1258(s), 1238(s), 1187 (s),1165(s),1141(s), 1093 (s), 1078(m),1060 (m), 1021(m),1002(m), 976(m), 890(w), 849(w),767(s), 745(s), 728 (m), 617 (s), 570(m). ^1H NMR [DMSO-d_6, 25 ^oC, 400 MHz; δ(ppm)]: 14.17 (s, 2H), 7.86–7.74 (m, 10H), 7.57–7.47 (m, 10H), 7.16 (s, 12H), 6.30 (t, *J*=2.0 Hz, 6H), 5.31 (s, 12H). ^{13}C NMR [DMSO-d_6, 25 ^oC, 400 MHz; δ(ppm)]: 167.6, 144.2, 139.5, 136.9, 131.1, 130.8, 130.6, 129.7, 127.7, 126.6, 105.7, 54.4.

Synthesis of {[Ag_2(bpmb)$_2$(3-sb)]·4H_2O}$_n$ (3)

This complex was prepared similarly to **2** except for the use of 3-NaHsb instead of 2-H_2sb. After cooling to the room temperature, a clear solution was obtained and then filtered. The resulting solution was allowed to evaporate in the dark. Two days later, colorless block crystals were collected by filtration. Yield: 75%. Anal. Calcd (%) for $C_{35}H_{40}N_8Ag_2SO_9$: C, 43.58; H, 4.15; N, 11.62. Found: C, 43.87; H, 4.01; N, 11.55. IR (KBr pellet, cm^{-1}): 3432 (s), 3116(m), 3090(m), 2934(w), 1600(s),1560(s), 1516(s), 1437(s), 1424(s), 1399(s), 1385(s), 1358(s), 1284(s), 1229(s), 1185(s), 1168(s), 1093 (s), 1050(s), 1037(s), 1020(m), 975(m), 915(m), 808(m), 767(s), 745(s), 668(m), 616 (s), 485(m). ^1H NMR [DMSO-d_6, 25 ^oC, 400 MHz; δ(ppm)]: 8.31 (m, *J*=1.6 Hz,1H), 7.92–7.88 (m, 5H), 7.68–7.66 (m, 1H), 7.51–7.50 (m, 4H), 7.33–7.30 (m, 1H), 7.16 (s, 8H), 6.33 (t, *J*=2.0 Hz, 4H), 5.34 (s, 8H). ^{13}C NMR [DMSO-d_6, 25 ^oC, 400 MHz; δ(ppm)]: 170.1, 147.6, 140.1, 136.7, 136.5, 131.1, 129.6, 127.8, 127.1, 127.0, 127.0, 106.0, 54.4.

Synthesis of {[Ag(bpmb)(4-Hsb)]·2H_2O}$_n$ (4)

A mixture of $AgNO_3$ (0.032 g, 0.20 mmol), 4-KHsb (0.047 g, 0.20 mmol), bpmb (0.045 g, 0.20 mmol) and distilled water (15 ml) was placed in a 30-mL Teflon lined stainless-steel reactor and heated at 423 K for two days. After cooling to the room temperature, colorless needle-shaped crystals were collected by filtration. Yield: 64%. Anal. Calcd (%) for $C_{21}H_{23}N_4AgSO_7$: C, 43.27; H, 3.94; N, 9.61. Found: C, 43.03; H, 3.86; N, 9.51. IR (KBr pellet, cm^{-1}): 3478(s), 3424 (s), 3134(m), 3116(m), 3090(m), 1701(s), 1654(m), 1636(m), 1513(m), 1437(m), 1424(m), 1400(s), 1358(m), 1285(s), 1185(s), 1136(m), 1094 (m), 1033(m), 1011(s), 975(m), 915(w), 767(s), 718(m), 636(s), 485(m). ^1H NMR [DMSO-d_6, 25 ^oC, 400 MHz; δ(ppm)]: 12.98 (s, 1H), 7.91–7.86 (m, 4H), 7.71–7.69 (m, 2H), 7.48–7.47 (m, 2H), 7.16 (s, 4H), 6.30 (t, *J*=2.0 Hz, 2H), 5.32 (s, 4H). ^{13}C NMR [DMSO-d_6, 25 ^oC, 400 MHz; δ(ppm)]: 167.0, 152.2, 139.5, 136.9, 130.6, 128.9, 127.7, 125.7, 105.7, 54.4.

X-ray Crystallographic Determination

Crystallographic data were collected at 295K on an Oxford Diffraction Xcalibur CCD diffractometer using graphite monochromated Mo-Kα radiation (λ = 0.71073 Å). The frames were integrated with the CrysAlisPro package and the data were corrected for absorption using the program CrysAlisPro.[37] The structures were solved by direct methods using the program SHELXL-97.[38] All non-hydrogen atoms were refined with anisotropic thermal parameters by full-matrix least-squares calculations on F^2 using the program SHELXL-97. The graphics were drawn by the ORTEP and Mercury.[39-40] Details of crystal data and structure refinements for the four complexes are listed in Table 4.

CCDC 958100-958103 for complexes **1-4** contain the supplementary crystallographic data for this paper. These data can be obtainined free of charge from the Cambridge Crystallographic Data Centre via www.ccdc.cam.ac.uk/data_request/cif.

Table 4 Crystallographic data and refinement parameters for the complexes **1-4**

Complex	**1**	**2**	**3**	**4**
Empirical Formula	$C_{98}H_{90}N_{20}O_{21}Ag_6S_4$	$C_{28}H_{26}N_6O_5AgS$	$C_{35}H_{40}N_8O_9Ag_2S$	$C_{21}H_{23}N_4O_7AgS$
Mr	2659.41	666.49	964.56	583.37
Crystal color /shape	Colorless/block	Colorless/plate	Colorless/block	Colorless/needle
Crystal system, space group	Triclinic, P-1	Triclinic, P-1	Triclinic, P-1	Triclinic, P-1
Crystal size	0.22×0.26×0.29	0.15×0.18×0.42	0.23×0.26×0.29	0.25×0.13×0.08
a/ Å	10.6768(4)	10.4087(4)	10.6331(3)	8.2280(4)
b/ Å	12.6832(4)	11.5583(5)	11.3717(3)	10.4465(5)
c/ Å	19.6770(9)	12.1619(6)	18.0884(5)	13.3444(7)
α/°	84.345(3)	88.778(4)	98.097(1)	92.427(1)
β/°	75.994(3)	72.109(4)	98.286(1)	90.631(1)
γ/°	76.864(3)	80.521(4)	113.971(1)	94.105(1)
Volume($Å^3$), Z	2515.04(17), 1	1372.73(11), 2	1928.99(9), 2	1142.92(10), 2
Calculated density($g·cm^{-3}$)	1.756	1.612	1.661	1.695
Absorption coefficient(mm^{-1})	1.310	0.861	1.133	1.024
F(000)	1332	678	976	592
Measured reflections	15742	8719	19941	9446
Unique reflections	8940	4869	6820	4005
Observed	6935	4263	6009	3413

reflections				
θ rang/°	3.2-25.1	3.0-25.1	1.2-25.1	1.5-25.1
parameters	695	370	520	322
Goodness-of-fit on F^2	1.030	1.000	1.065	1.090
R_1 and ωR_2 (I>2σ(I))	0.040, 0.090	0.032,0.076	0.038, 0.107	0.032, 0.095
R_1 and ωR_2(all data)	0.058, 0.099	0.040, 0.082	0.044, 0.117	0.042, 0.118
Largest peak and hole(e· Å^{-3})	0.948, -0.668	0.855, -0.503	1.173, -0.748	0.527, -0.636

Catalytic Oxidation of Methyl Phenyl Sulfide

The synthesized complex as a catalyst (0.015 mmol) was mixed with 5 mL ethanol in a 25 mL round-bottom glass-reactor, and then the methyl phenyl sulfide (0.5 mmol) was added. The mixture was kept at 323K under stirring, and the hydrogen peroxide (1.5 mmol) then was introduced as the oxidant. At the same time the initial reaction time was recorded. The experiments were performed by two methods. One is in the absence of the 2-H_2sb while the other is in the presence of 2-H_2sb (0.0021 g, 0.01 mmol). The reaction progress was monitored by GC. Assignments of products were made by comparison with authentic samples. All the reactions were run at least in duplication.

Supporting Information (see footnote on the first page of this article): IR spectra of complexes **1-4**. Representative GC chromatograms. ^{1}H NMR for bpmb. ^{1}HNMR and ^{13}C NMR for complexes **1-4**. Extended hydrogen-bonding patterns for complexes 1-4. XRD patterns and simulated ones by single crystal data of complexes **1-4** and XRD patterns of complex **2** after the recycle of catalytic reaction.

Acknowledgment

The authors thank the National Natural Science Foundation of China (grant No. 21073157).

Notes and references

1 G. R. Desiraju, *J. Am. Chem. Soc.,* 2013, *135*, 9952-9967; M. Du, C. P. Li, C. S. Liu and S. M. Fang, *Coord. Chem. Rev.,* 2013, *257*, 1282-1305; R. Patra, H. M. Titi and I. Goldberg, *Cryst. Growth & Des.,* 2013, *13*, 1342-1349.

2 S. H. Park, S. Y. Lee, K. M. Park and S. S. Lee, *Acc. Chem. Res.,* 2012, *45*, 391-403; Y. Y. Xu, Y. Y. Xing, X. Y. Duan, Y. Z. Li, H. Z. Zhu and G. J. Meng, *CrystEngComm,* 2010, *12*, 567-572.

3 X. L. Tong, H. L. Lin, J. H. Xin, F. Liu, M. Li and X. P. Zhu, *J. Nanomaterials,* 2013, DOI: 10.1155/2013/616501; M. Clemente-Leon, E. Coronado, C. Marti-Gastaldo and F. M. Romero, *Chem. Soc. Rev.,* 2011, *40*, 473-497; D. Braga,

F. Grepioni, *Acc. Chem. Res.,* 2000, *33*, 601-608.

4 N. C. Burtch, H. Jasuja, D. Dubbeldam and K. S. Walton, *J. Am. Chem. Soc.,* 2013, *135*, 7172-7180; K. Sumida, D. Stuck, L. Mino, J. D. Chai, E. D. Bloch, O. Zavorotynska, L. J. Murray, M. Dinca, S. Chavan, S. Bordiga, M. Head-Gordon and J. R. Long, *J. Am. Chem. Soc.,* 2013, *135*, 1083-1091; J. R. Li, Y. G. Ma, M. C. McCarthy, J. Sculley, J. M. Yu, H. K. Jeong, P. B. Balbuena and H. C. Zhou, *Coord. Chem. Rev.,* 2011, *255*, 1791-1823; A. C. McKinlay, R. E. Morris, P. Horcajada, G. Ferey, R. Gref, P. Couvreur and C. Serre, *Angew. Chem. Int. Ed.,* 2010, *49*, 6260-6266.

5 S. Nakagaki, G. K. B. Ferreira, G. M. Ucoski and K. A. D. D. Castro, *Molecules,* 2013, *16*, 7279-7308; C. D. Wu and W. B. Lin, *Angew. Chem. Int. Ed.,* 2007, *46*, 1075-1078; D. Farrusseng, S. Aguado and C. Pinel, *Angew. Chem. Int. Ed.,* 2009, *48* (41), 7502-7513.

6 A. O. Ibrahim, Y. F. Zhou, F. L. Jiang, L. Chen, X. J. Li, W. T. Xu, O. O. E. Onawumi, O. A. Odunota and M. C. Hong, *Eur. J. Inorg. Chem.,* 2011, *(32)*, 5000-5005; I. Goldberg, *CrystEngComm,* 2008, *10*, 637-645; J. R. Li, R. J. Kuppler and H. C. Zhou, *Chem. Soc. Rev.,* 2009, *38*, 1477-1480.

7 H. L. Jiang and Q. Xu, *Chem. Comm.,* 2011, *47*, 3351-3370; B. Chen, L. Wang, Y. Xiao, F. R. Fronczek, M. Xue, Y. Cui and G. Qian, *Angew. Chem. Int. Ed.,* 2009, *48*, 500-503.

8 A. A. Massoud, V. Langer, Y. M. Gohar, M. A. M. Abu-Youssef, J. Janis, G. Lindberg, K. Hansson and L. Ohrstrom, *Inorg. Chem.,* 2013, *52*, 4046-4060; J. Malberg, T. Wiegand, H. Eckert, M. Bodensteiner and R. Wolf, *Chem. Eur. J.,* 2013, *19*, 2356-2369; D. Venkataraman, Y. Du, S. R. Wilson, K. A. Hirsch, P. Zhang and J. S. Moore, *J. Chem. Edu.,* 1997, *74*, 915-918.

9 M. Maekawa, T. Miyazaki, K. Sugimoto, T. Okubo, T. Kuroda-Sowa, M. Munakata and S. Kitagawa, *Dalton Trans.,* 2013, *42*, 4258-4266; L. Tei, V. Lippolis, A. J. Blake, P. A. Cooke and M. Schroder, *Chem. Comm.,* 1998, *(23)*, 2633-2634.

10 F. R. Knight, R. A. M. Randall, L. Wakefield, A. M. Z. Slawin and J. D. Woollins, *Dalton Trans.,* 2013, *42*, 143-154; A. N. Khlobystov, A. J. Blake, N. R. Champness, D. A. Lemenovskii, A. G. Majouga, N. V. Zyk and M. Schroder, *Coord. Chem. Rev.,* 2001, *222*, 155-192.

11 H. R. Khavasi and B. M. M. Sadegh, *Cryst. Growth & Des.,* 2012, *12*, 4798-4804; X. P. Li, J. Y. Zhang, M. Pan, S. R. Zheng, Y. Liu and C. Y. Su, *Inorg. Chem.,* 2007, 46, 4617-4625.

12 C. L. Chen, B. S. Kang and C. Y. Su, *Aust. J. Chem.* 2006, *59*, 3-18; C. A. Hollis, S. R. Batten and C. J. Sumby, *Cryst. Growth & Des.,* 2013, *13*, 2350-2361; X. F. Zheng and L. G. Zhu, *J. Mol. Struct.,* 2013, *1039*, 1-7.

13 C. Y. Su, Y. P. Cai, C. L. Chen, M. D. Smith, W. Kaim and H. C. zur Loye, *J. Am. Chem. Soc.,* 2003, *125*, 8595-8613; B. Li, S. Q. Zang, H. Y. Li, Y. J. Wu and T. C. W. Mak, *J. Organomet. Chem.,* 2012, *708*, 112-117.

14 M. C. Brandys and R. J. Puddephatt, *J. Am. Chem. Soc.,* 2002, *124*, 3946-3950; B. Notash, N. Safari and H. R. Khavasi, *CrystEngComm,* 2012, *14*, 6788-6796; J. L.

Gulbransen and C. M. Fitchett, *CrystEngComm,* 2012, *14*, 5394-5397.

15 X. F. Zheng and L. G. Zhu, *Cryst. Growth & Des.,* 2009, 9, 4407-4417.

16 X. F. Zheng and L. G. Zhu, *Polyhedron,* 2011, 30, 666-675.

17 X. H. Miao and L. G. Zhu, *Dalton Trans.,* 2010, 39, 1457-1459.

18 P. Thuery, *Inorg. Chem.* 2013, *52*, 435-447; B. F. Hoskins, R. Robson and D. A. Slizys, *J. Am. Chem. Soc.,* 1997, *119*, 2952-2953; S. Song, X. Li and Y. H. Zhang, *Dalton Trans.,* 2013, *42*, 10409-10412.

19 P. Thuery, *Cryst. Growth & Des.,* 2011, *11*, 5702-5711; P. Thuery, *Cryst. Growth & Des.,* 2012, *12*, 1632-1640; S. Chawla, M. Arora, K. Nattinen, K. Rissanen and J. V. Yakkmi, *Polyhedron,* 2004, 23, 3007-3019; X. F. Li, Y. B. Huang and R. Cao, *Dalton Trans.,* 2012, *41*, 6195-6205.

20 X. H. Miao and L. G. Zhu, *CrystEngComm,* 2009, *11*, 2500-2509.

21 N. Khiar, V. Valdivia, A. Salvador, A. Chelouan, A. Alcudia and I. Fernandez, *Adv. Synth. & Cata.,* 2013, *355*, 1303-1307; N. Salam, P. Mondal, J. Mondal, A. S. Roy, A. Bhaumik and S. M. Islam, *RSC Advances,* 2012, *2*, 6464-6477.

22 E. Wojaczyńska and J. Wojaczyński, *Chem. Rev.,* 2010, *110*, 4303-4356; W. L. Li, Z. G. Xie and X. B. Jing, *Cata. Comm.,* 2011, *16*, 94-97.

23 J. Legros, J. R. Dehli and C. Bolm, *Adv. Synth. & Cata.,* 2005, *347*, 19-31; A. Toutchkine and E. L. Clennan, *J. Org. Chem.,* 1999, *64*, 5620-5625.

24 H. L. Holland, *Natural Product Reports,* 2001, *18*, 171-181.

25 I. Fernandez and N. Khiar, *Chem. Rev.,* 2003, *103*, 3651-3705.

26 R. Das and D. Chakraborty, *Synthesis,* 2011, (2), 277-280.

27 M. K. Nazeeraddin, S. M. Zakeeruddin and K. Kalyanasundaran, *J. Phys. Chem.,* 1993, *97*, 9607-9612; X. Y. Qian, J. L. Song and J. G. Mao, *Inorg. Chem.,* 2013, *52*, 1843-1853; A. Spangenberg, J. P. Malval, H. Akdas-Kilig, J. L. Fillaut, F. Stehlin, N. Hobeika, F. Morlet-Savary and O. Soppera, *Macromolecules,* 2012, *45*, 1262-1269.

28 C. Seward, J. Chan, D. Song and S. Wang, *Inorg. Chem.,* 2003, *42*, 1112-1120; H. H. Zhang, W. Dou, W. S. Liu, X. L. Tang and W. W. Qin, *Eur. J. Inorg. Chem.,* 2011, *(5)*, 748-753.

29 K. Akhbari, A. Morsali and L. G. Zhu, *J. Mol. Struct.,* 2008, *891*, 132-137.

30 M. C. Aragoni, M. Arca, F. Demartin, F. A. Devillanova, F. Isaia, A. Garau, V. Lippolis, F. Jalali, U. Papke, M. Shamsipur, L. Tei, A. Yari and G. Verani, *Inorg. Chem.,* 2002, *41*, 6623-6632.

31 S. L. Zheng, M. Gembicky, M. Messerschmidt, P. M. Dominiak and P. Coppens, *Inorg. Chem.,* 2006, *45*, 9281-9289.

32 S. L. Zheng and P. Coppens, *Crystal Growth & Des.,* 2005, *5*, 2050-2059.

33 W. T. Hu and L. G. Zhu, *Chin. J. Inorg. Chem.,* 2013, *29*, 1109-1114.

34 M. R. Maurya, B. Singh, P. Adao, F. Avecilla and J. C. Pessoa, *Eur. J. Inorg. Chem.*, 2007, 5720-5734.

35 W. T. Hu and L. G. Zhu, *J. Coord. Chem.*, 2013, *66*, 3045-3057.

36 E. A. Nudnova, A. S. Potapov, A. I. Khlebnikov and V. D. Ogorodnikov, *Russ. J. Org. Chem.,* 2007, *43*, 1698-1702.

37 *CrysAlisPro*, Version 1.171.33.52, Oxford Diffraction Ltd., 2009.

38 G. M. Sheldrick, SHELXL-97, program for crystal structure refinement, University of Göttingen, Göttingen, Germany, 1997.

39 L. J. Farrugia, *J. Appl. Crystallogra.,* 1999, *32,* 837-838.

40 C. F. Macrae, P. R. Edgington, P. McCabe, E. Pidcock, G. P. Shields, R. Taylor, M. Towler and J. van de Streek, *J. Appl. Cryst.,* 2006, *39*, 453-457.

Graphical Abstract

Diverse Silver(I) Sulfobenzoate Coordination Polymers and their Recycling property as Homogeneous Catalyst in Oxygenation of Sulfide

Ai-Qing Ma and Long-Guan Zhu*
Department of Chemistry, Zhejiang University, Hangzhou 310027, People's Republic of China
E-mail:chezlg@zju.edu.cn

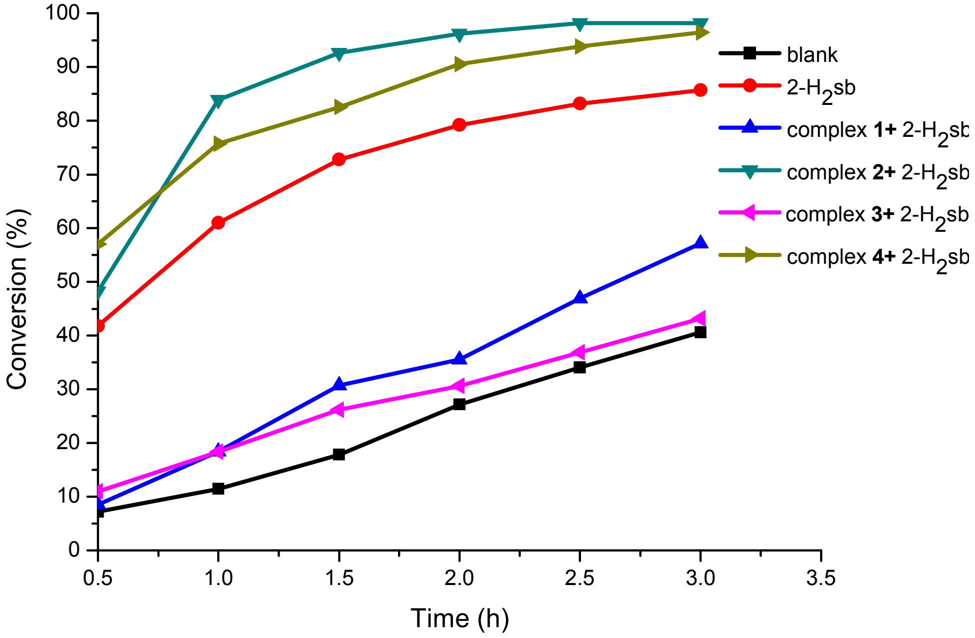

Four diverse silver sulfobenzoate coordination polymers with 1,4-bis(pyrazolyl-methyl)-benzene ligands were prepared. Diverse structures differ with respect to molecular conformation, coordination modes of sulfobenzoates, and weak interactions. In addition, the catalytic activity to selective oxidation of methyl phenyl sulfide with H_2O_2 to sulfoxide revealed that complex **2** is a homogeneous catalyst during the catalytic reaction while it can be recovered by filtration upon cooling and then reused at least four times without losing activity.